



# The Kinematic Analysis and Evolution of the Stress Fields in the Zagros Foreland Folded Belt, Fars Salient, Iran

Bahareh Zafarmand <sup>1\*</sup>, Khalil Sarkarinejad <sup>2</sup>

<sup>1\*</sup> PhD, Department of Earth Science, College of Sciences, Shiraz University, Shiraz, Iran.

(bahar\_zafarmand@yahoo.com)

<sup>2</sup> Professor, Department of Earth Science, College of Sciences, Shiraz University, Shiraz, Iran.

(Date of received: 03/09/2020, Date of accepted: 16/11/2020)

## ABSTRACT

The NW-SE trending Zagros Orogenic Belt was initiated during the convergence of the Afro-Arabian continent and the Iranian microcontinent in the Late Cretaceous. Ongoing convergence is confirmed by intense seismicity related to compressional stresses collision-related in the Zagros Orogenic Belt by reactivation of an early extensional faulting to latter compressional segmented strike-slip and dip-slip faulting. These activities are strongly related either to the deep-seated basement fault activities (deep-seated earthquakes) underlies the sedimentary cover or gently dipping shallow-seated décollement horizon of the rheological weak rocks of the Infra-Cambrian Hormuz salt. The Compressional stress regimes in the different units plays an important role in controlling the stress conditions between the different units within the sedimentary cover and basement. A significant set of nearly N-S trending right-lateral strike-slip faults exists throughout the study area in the Fars area in the Zagros Foreland Folded Belt. Fault-slip and focal mechanism data, were analyzed using the stress inversion method to reconstruct the paleo and recent stress conditions. The results suggest that the current direction of maximum principal stress averages N19°E, with N38°E that for the past from Cretaceous to Tertiary, (although a few sites on the Kar-e-Bas fault yield a different direction). The results are consistent with the collision of the Afro-Arabian continent and the Iranian microcontinent. The difference between the current and paleo-stress directions indicates an anticlockwise rotation in the maximum principle stress direction over time. This difference resulted from changes in the continental convergence path, but was also influenced by the local structural evolution, including the lateral propagation of folds and the presence of several local décollement horizons that facilitated decoupling of the deformation between the basement and sedimentary cover. The obliquity of the maximum compressional stress into the fault trends reveal a typical stress partitioning of thrust and strike-slip motion in the Kazerun, Kar-e-Bas, Sabz-Pushan, and Sarvestan fault zones, that caused these fault zones behave as segmented strike-slip and dip-slip faults (Sarkarinejad et al., 2018).

## Keywords:

Fault-slip data; Earthquake focal mechanism; Paleo-stress; Recent tectonic stress; Zagros.



## 1. Introduction

There are some critical questions about the relationship between the stress regime during the initiation of the Zagros orogenic belt and its later evolution. For example, as in some other collisional orogens like Himalaya-Tibet orogen, is the compressional direction almost parallel to the plate motion? What is the variation in the orientation of the principal stresses over time? Previous work (e.g. Vernant et al., 2004 [1]; McQuarrie et al., 2003 [2]) suggested that the convergence path between the Iranian microcontinent and the Afro-Arabian continent from the Mesozoic to the Recent has been oblique and is deviated from N-E to the N. Is there data to support these proposed compressional trends over time? The deformation in the sedimentary cover is decoupled from the basement (likely at the level of the Hormuz salt). Is there any variation in the stress direction between the sedimentary cover and the upper gneissic crust? Unlike the locations of the studies by Lacombe et al. (2006) [3] and Navabpour et al. (2007) [4], the locations chosen in our study were close to fault zones. In the vicinity of the main lateral fault zones (e.g., Kazerun and Kar-e-Bas fault zones), is the stress regime similar to that in other parts of the Zagros orogenic belt? In other words, is there any significant deviation of compressional direction in the vicinity of the major lateral fault zone? This work will have a far reaching implication in seismicity of the Zagros Orogenic Belt.

In this study, we inferred the paleo and recent stress regimes based on the inversion of fault-slip data and earthquake focal mechanisms. We also used these results to test the role of the Infra-Cambrian Hormuz salt (Mukherjee 2013 [5]) as a décollement horizon between the sedimentary cover and the basement by comparing the results of the inversion of the fault slip and earthquake focal mechanism data. The Fars area is a key region to understand the tectonic and kinematic evolution of the Zagros Orogenic Belt from the Cenozoic to the recent times. The study area is located in the central part of the Zagros Foreland Folded Belt (F-FOB) in the Fars salient (Figure 1). To evaluate the possible stress variations along the trend of the orogen from the northwest to the southeast, the study area extends from the Kazerun to the Sarvestan fault zones (Figure 1).

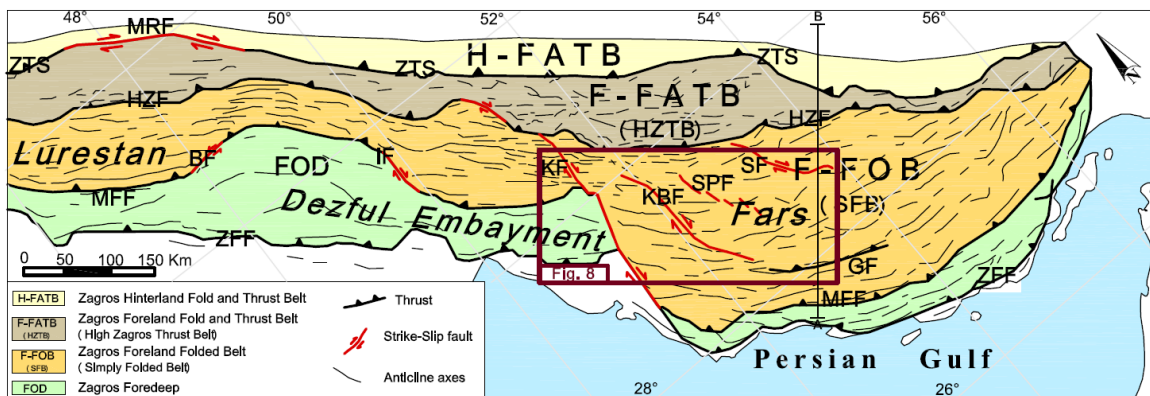


**Figure. 1** Structural map and subdivision of the Iranian sector of the Zagros Orogenic Belt and location of the major fault zones including the study area, (modified from Huber, 1977 [6]; Berberian, 1995 [7]; Sepehr and Cosgrove, 2005 [8]; Sarkarinejad and Ghanbarian, 2014 [9]; Sarkarinejad and Zafarmand, 2017a,b [10-11]). H-FATB: Zagros Hinterland Fold and Thrust Belt, F-FATB: Zagros Foreland Fold and Thrust Belt, F-FOB: Zagros Foreland Folded Belt, FOD: Zagros Foredeep, ZTS: Zagros Thrust System, MRF: Main Recent fault, HZF: High Zagros fault, MFF: Mountain Front fault, ZFF: Zagros Foredeep fault, BF: Balarud fault, IF: Izeh fault, KF: Kazerun fault, KBF: Kar-e-Bas fault, SPF: Sabz-Pushan fault, SF: Sarvestan fault, GF: Ghir fault. The AB black line indicates the cross-section path of Figure 3.



## 2. Tectonic and seismotectonic settings

The Zagros Orogenic Belt is the result of still continuing continent-continent collision between the Iranian microcontinent and the Afro-Arabian continent which probably started in the Late Cretaceous and developed during the Mio-Pliocene times (Falcon, 1974 [12]; Berberian and King, 1981 [13]; Alavi, 1994 [14]; Molinaro et al., 2005 [15], Lacombe et al., 2006 [16]; Aubourg et al., 2010 [17]). The convergence of the Afro-Arabian continent with the Iranian microcontinent trends N-S to NNE, with a convergence velocity ranging from 23 (Bayer et al., 2003 [18]) to 35 mm yr<sup>-1</sup> (DeMets et al., 1990 [19]) (Figure. 2). The NE-trending shortening rate increases from the northwest to the southeast, up to approximately 10 mm yr<sup>-1</sup> (Tatar et al., 2002 [20]; Vernant et al., 2004 [1]). Some active transverse or cross-faults within the Zagros Orogenic Belt, such as the Kazerun, Kar-e-Bas, Sabz-Pushan and Sarvestan faults, trend nearly north-south, at a high angle to the structural trend of the orogenic belt, whereas other faults, such as the High Zagros and Mountain Front faults, trend NW-SE, sub-parallel to the belt. Right lateral strike-slip faults cut across the trend of the belt and terminate as thrusts parallel to the folds (Figures. 1 and 2). The lateral fault zones through the Zagros Orogenic Belt play a major kinematic role by accommodating the change in shortening, which is partitioned in the western central Zagros and non-partitioned in the eastern Zagros (Yamini Fard et al., 2006 [21]).

Sarkarinejad and Ghanbarian (2014) [9] introduced new terminology that relates to Zagros Orogenic Belt. They suggested that the Zagros Orogenic Belt could be divided into seven major belts. In this paper we modified these divisions and introduce the new division that divides Zagros Orogenic Belt into nine sub-parallel tectonic belts; These include from SW to NE: 1- Zagros Foreland Folded Belt; 2- Zagros Foreland Fold-and-Thrust Belt; 3- Zagros Thrust System; 4- Zagros Suture Zone / Ophiolite Zone; 5- Slate Belt; 6- Zagros Hinterland Fold-and-Thrust Belt; 7- Sanandaj-Sirjan HP-LT Metamorphic Belt; 8- HT-LP Metamorphic Belt; 9- Urumieh-Dokhtar Magmatic Belt (Figure 3). The Infra-Cambrian Hormuz salt in the Fars area lies on top of the basement and served as the major décollement horizon during the Late Tertiary deformation. Other décollement horizons include the Triassic Dashtak Formation (evaporites), the Cretaceous Kazhdumi Formation (shale), and the lower Miocene Gachsaran Formation (evaporites). These décollement horizons decoupled deformation between the basement and sedimentary cover and also between different units within the sedimentary cover.

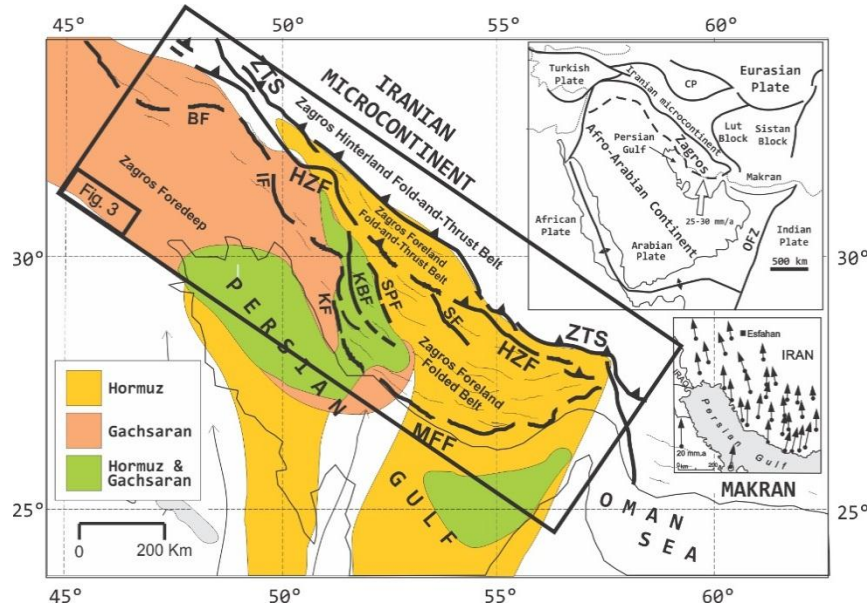


**Figure. 2** Structural map of the central Zagros Orogenic Belt showing geographic extent of the Gachsaran and Hormuz evaporitic facies (Sherkati and Letouzey, 2004 [22]; Oveisi et al., 2009 [23]). ZTS: Zagros Thrust System, HZF: High Zagros Fault, MFF: Mountain Front Fault, BF: Bala Rud fault zone, IF: Izeh fault zone, KF: Kazerun fault zone, KSF: Kar-e-Bas fault zone, SBZ: Sabz-Pushan fault zone, SF: Sarvestan fault. Upper right inset diagram shows the Afro-Arabian continent and the Iranian microcontinent. White arrow shows 25-30 mm/yr motion of the Afro-Arabian continent relative to the Eurasian continent. Lower right inset shows GPS velocities (mm/yr) in the central Zagros with respect to stable Eurasia (Hessami et al., 2006 [24]). This map is modified from Sarkarinejad and Ghanbarian (2014) [9].

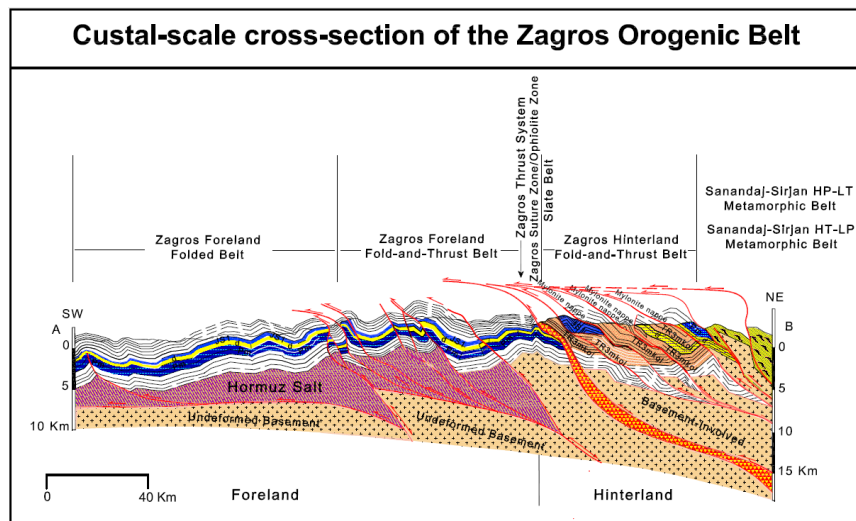


**Figure. 3** Crustal-scale cross section of the Zagros Orogenic Belt (divisions are modified from Sarkarinejad and Azizi, 2008 [25]; Sarkarinejad and Ghanbarian, 2014 [9]); from SW to NE: (1) Zagros Foreland Folded Belt; (2) Zagros Foreland Fold-and-Thrust Belt; (3) Zagros Thrust System (ZTS); (4) Zagros suture zone / Ophiolite zone; (5) Slate Belt; (6) Zagros hinterland Fold-and-Thrust Belt; (7) Sanandaj-Sirjan HP-LT metamorphic Belt; (8) Sanandaj-Sirjan HT-LP metamorphic Belt; (9) Urumieh-Dokhtar magmatic Belt.





### 3. Inversion of Earthquake Focal Mechanism and Fault-Slip Data

To reconstruct the paleo and recent stress states within the study area, we applied two methods: 1) Inversion of the earthquake focal mechanisms and 2) inversion of fault-slip data. To determine the present-day stress pattern in the western Fars, we used inversion of the earthquake focal mechanisms described by previous studies (McKenzie, 1969 [26]; Otsubo et al., 2008 [27]; Yamaji et al., 2011 [28]). Fault-slip analyses and paleostress methods are commonly applied to infer different phases of extension and shortening (Angelier et al., 1990 [29]; Zalohar and Vrabec, 2007 [30]). We applied inversion of the slickenlines on fault planes to constrain the stresses responsible for older phases of deformation. Both of these methods are based on the Wallace–Bott hypothesis that expresses the slip vector of an earthquake as parallel to the resolved shear stress on the fault (Wallace, 1951 [31]; Bott, 1959 [32]). The fault-slip inversion method assumes that (1) the rock body is mechanically homogeneous and isotropic; (2) the rock has a linear viscous rheology (Twiss and Unruh, 1998 [33]; Lacombe, 2012 [3]); (3) displacements on the fault planes are small with respect to their lengths and there is no ductile deformation and, thus, no rotation of the fault planes; (4) a tectonic event is characterized by a single homogeneous stress tensor; (5) the fault plane is a pre-existing fracture and the slip responsible for the slickenlines occurs in the direction of maximum resolved shear stress; and (6) the slip on each fault plane is independent of the slip on all other fault planes. To infer the present-day state of stress in the Fars salient, we applied the stress inversion method to the focal mechanism data. The data are the azimuth and dip of two nodal planes and the rake of the lineations. The stress inversion methods assume a uniform state of stress. To interpolate the P- and T- axes (approximations of maximum and minimum principal stress directions), the method yields the principal stress axes and ratio between the principal stress magnitudes. The misfit angle is the angle between the measured slickenlines and the calculated relative shear stress,  $\tau$ . The basic principle of inversion of slip data involves finding the best fit between the observed directions and senses of slip on the numerous faults and theoretical shear stress on these planes. Similar to the inversion of the earthquake focal mechanisms, the results are reported as the trend and plunge of the three principal stress axes,  $\sigma_1$ ,  $\sigma_2$ , and  $\sigma_3$ , and the ratio  $\Phi = (\sigma_2 - \sigma_3)/(\sigma_1 - \sigma_3)$ , which describes the shape of the stress ellipsoid and thus the nature of the stress regime (for example, if  $\sigma_3$  is vertical and  $\Phi$  close to 0, it is a reverse/strike-slip regime) (Bott's, 1959 [32]; Fossen, 2016 [34]).

## 4. Results of Stress Analyses

### 4.1. Earthquake focal mechanism inversion

Because earthquakes with higher magnitudes yield more accurate nodal plane locations and geometries (e.g., Hatzfeld, 1999 [35] and Maggi et al., 2002 [36]), we have used earthquakes with moment magnitudes  $M_w \geq 4.2$  in our analysis. Most of the thrust earthquakes (between 1968 to 2000, Talebian and Jackson, 2004 [37]) occur along the SW Zagros margin, between the coastal plain of the Persian Gulf and the Surmeh-Ghir thrust system while the strike-slip earthquakes are closely associated with the Kar-e-Bas and Sabz-Pushan fault zones (Lacombe et al., 2006 [16]). The Kazerun fault zone has both compressional dip-slip and strike-slip motion, and the Ghir fault zone is dominantly compressional dip-slip. Because the seismicity in the central Zagros is beneath the sedimentary cover and in the upper part of the basement (Tatar et al., 2004 [38] and Hatzfeld et al., 2010 [39]), the results obtained from inversion of the focal mechanism refer to the foreland gneissic



basement. The results of earthquake focal mechanism inversion have been shown in Table 1 and Figure 4.

**Table 1. Results of inversion of the earthquake focal mechanisms.  $T\sigma_1$  and  $P\sigma_1$  indicate trend and plunge of maximum compression, and  $T\sigma_3$  and  $P\sigma_3$  represent trend and plunge of minimum compression.  $\Phi$  is the shape ratio (Sarkarinejad et al., 2018 [40])**

| location         | $T\sigma_1$ | $P\sigma_1$ | $T\sigma_3$ | $P\sigma_3$ | $\Phi$ |
|------------------|-------------|-------------|-------------|-------------|--------|
| Kazerun Fault    | S46°W       | 09°         | N42°W       | 09°         | 0.04   |
| Kar-e-Bas Fault  | N26°E       | 08°         | N65°W       | 08°         | 0.72   |
| SabzPushan Fault | N00°E       | 08°         | S88°E       | 08°         | 0.6    |
| Ghir fault       | N05°E       | 04°         | S63°W       | 83°         | 0.88   |

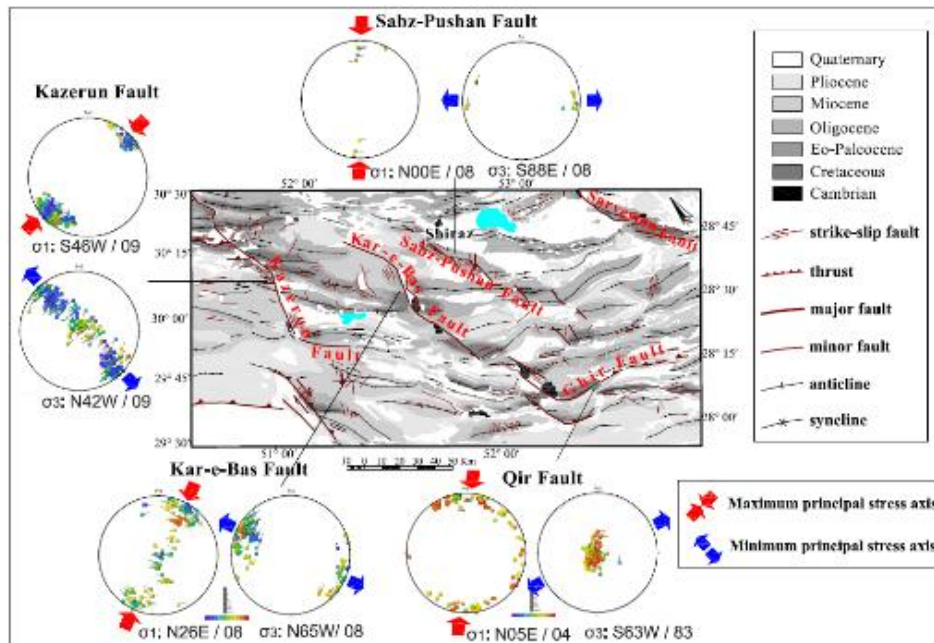


**Figure 4.** Geological map of the study area showing maximum and minimum principal stress orientations based on inversion of earthquake focal mechanism data for each fault zone (Sarkarinejad et al., 2018 [40])

#### 4.2. Fault slip inversion

To evaluate the paleostress regime of the Kazerun, Kar-e-Bas, Sabz-Pushan, Sarvestan and Ghir fault zones, we defined suitable sites along each fault and measured the strike and dip of the fault plane, rake of the slickenline, and polarity of movement for each one in the field. For more accuracy, all measurements have been done with Brunton compass. In each fault zone, the number of sites and measurements is shown in Table 2. According to field observations and Anderson (1951) [41], the fault systems in sites 10 and 11 in the Sarvestan fault zone and sites 12, 13, and 14 in the Ghir fault zone were back tilted prior to interpretation and analysis. Varied stress regimes are specified by different orientations of the principal stress axes. The inversion of the fault slip



data for the study area revealed stress regimes varying from compressional to tensional dip-slip and strike-slip for the Kazerun, Kar-e-Bas, Sabz-Pushan, Sarvestan, and Ghir fault zones. Table 2 and Fig. 5 show the results of the analysis for each fault zone in the study area.

**Table 2. Results of inversion of fault slip data.  $T\sigma_1$ ,  $P\sigma_1$ ,  $T\sigma_2$ ,  $P\sigma_2$ ,  $T\sigma_3$  and  $P\sigma_3$  represent the trend and plunge of the principal stresses ( $\sigma_1$ ,  $\sigma_2$ ,  $\sigma_3$  respectively).  $\Phi$  is the shape ratio and  $\alpha$  is the misfit angle. b : the sites were back tilted before interpretation (see Figure. 5).**

| site no. | site                                  | latitude    | longitude   | Formation | number of data | $T\sigma_1$ | $P\sigma_1$ | $T\sigma_2$ | $P\sigma_2$ | $T\sigma_3$ | $P\sigma_3$ | $\Phi$ | $\alpha$ |
|----------|---------------------------------------|-------------|-------------|-----------|----------------|-------------|-------------|-------------|-------------|-------------|-------------|--------|----------|
| 01       | Kazerun1,Normal Fault                 | 29° 56' 16" | 51° 35' 10" | Sarvak    | 9              | 220         | 78          | 332         | 05          | 063         | 12          | 0.1    | 14       |
| 01       | Kazerun1,Strike-Slip Fault            | 29° 56' 16" | 51° 35' 10" | Sarvak    | 9              | 260         | 35          | 074         | 55          | 168         | 03          | 0.5    | 7        |
| 02       | Kazerun2,Normal Fault                 | 29° 58' 40" | 51° 34' 19" | Sarvak    | 5              | 017         | 69          | 270         | 06          | 177         | 20          | 0.3    | 3        |
| 02       | Kazerun2,Strike-Slip Fault            | 29° 58' 40" | 51° 34' 19" | Sarvak    | 18             | 031         | 05          | 250         | 84          | 121         | 04          | 0.5    | 16       |
| 03       | Tang-e-Abulhayat,Strike-Slip Fault    | 29° 38' 33" | 51° 47' 23" | Asmari    | 16             | 031         | 13          | 273         | 64          | 124         | 22          | 0.2    | 14       |
| 04       | Tang-e-Abulhayat,Thrust Fault         | 29° 38' 15" | 51° 47' 30" | Asmari    | 7              | 228         | 04          | 138         | 01          | 027         | 87          | 0.6    | 10       |
| 05       | Kar-e-Bas1,Normal Fault               | 28° 54' 55" | 52° 16' 22" | Pabdeh    | 8              | 291         | 67          | 028         | 03          | 119         | 24          | 0.3    | 7        |
| 06       | Kar-e-Bas1,Strike-Slip Fault          | 28° 54' 32" | 52° 17' 13" | Asmari    | 7              | 043         | 22          | 207         | 67          | 311         | 06          | 0.2    | 7        |
| 07       | Kar-e-Bas2 Fault                      | 29° 27' 16" | 52° 09' 26" | Asmari    | 23             | 311         | 02          | 197         | 86          | 041         | 04          | 0.3    | 17       |
| 08       | SabzPushan,Strike-Slip Fault          | 29° 12' 13" | 52° 35' 49" | Asmari    | 9              | 199         | 19          | 026         | 71          | 292         | 01          | 0.4    | 14       |
| 09       | SabzPushan,Thrust Fault               | 29° 12' 15" | 52° 35' 47" | Asmari    | 40             | 018         | 08          | 288         | 05          | 167         | 80          | 0.8    | 7        |
| 10       | Sarvestan,Sinstral Fault <sup>b</sup> | 29° 00' 46" | 53° 19' 21" | Asmari    | 5              | 355         | 06          | 101         | 67          | 261         | 21          | 0.1    | 3        |
| 10       | Sarvestan,Dextral Fault <sup>b</sup>  | 29° 00' 46" | 53° 19' 21" | Asmari    | 10             | 233         | 27          | 001         | 50          | 129         | 27          | 0.3    | 8        |
| 11       | Sarvestan,Thrust Fault <sup>b</sup>   | 29° 00' 46" | 53° 19' 22" | Asmari    | 5              | 224         | 20          | 315         | 02          | 050         | 71          | 0.5    | 2        |
| 12       | Ghir,Strike-Slip Fault <sup>b</sup>   | 28° 34' 17" | 52° 58' 55" | Asmari    | 16             | 024         | 00          | 293         | 70          | 112         | 20          | 0.2    | 13       |
| 13       | Ghir,Thrust Fault <sup>b</sup>        | 28° 34' 18" | 52° 58' 54" | Asmari    | 8              | 042         | 06          | 309         | 24          | 145         | 65          | 0.2    | 5        |
| 14       | Ghir,Normal Fault <sup>b</sup>        | 28° 34' 17" | 52° 58' 54" | Asmari    | 7              | 152         | 56          | 300         | 29          | 039         | 16          | 0.3    | 13       |

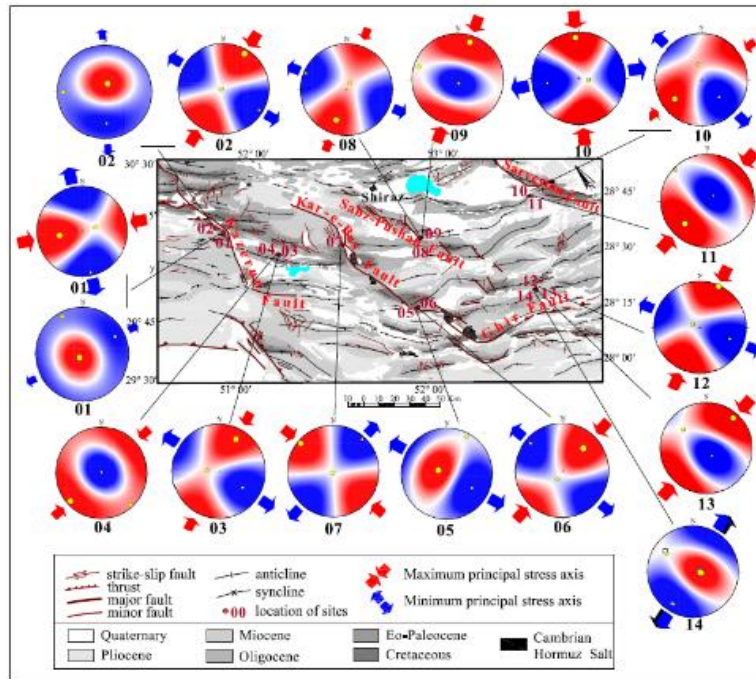


Figure 5. Stress orientations from inversion of fault slip data. Site numbers are listed below the spheres (Sarkarinejad et al., 2018 [40])

## 5. Discussion

The stress regimes obtained by inverting the fault-slip data may be local or regional. Only results that are consistent throughout the entire area can be considered tectonic regimes (Lacombe et al., 2006). Thus, the results obtained from the sites with a small spread of slickenlines have been eliminated. In each fault zone (Kazerun, Kar-e-Bas, Sabz-Pushan, Sarvestan, and Ghir fault zones), the inversion of both the earthquake focal mechanisms and fault slip data provide information regarding the temporal and spatial changes in the tectonic stress regime in the study area (Tables 1 and 2). These results allow us to illustrate changes in the direction of the principal compressional stress from older deformation to the most recent deformation (Figs. 4 and 5). The inversion of the earthquake focal mechanisms shows that the present day compressional direction averages  $\sim N19^\circ E$  and is compatible with the general direction of the recent convergence between the Afro-Arabian and Eurasian continents ( $\sim N13^\circ E$  at the longitude of  $52^\circ E$ , Vernant et al., 2004 [1]). From NW to SE (from Kazerun to Ghir fault zone), the spatial variation in the recent compressional trend has a counterclockwise rotation. This rotation is consistent with the spatial change of the Afro-Arabian–Eurasian convergence paths along the Zagros Orogenic Belt that has been previously suggested (e.g., Vernant et al., 2004 [1]; Walpersdorf et al., 2006 [42]). On the other hand, the fault slip data produce an average trend of  $\sim N38^\circ E$  for the paleo-compression direction. The relative consistency of the results from the inversion of the focal mechanisms and the fault-slip data also suggests that there is not a significant temporal variation in the direction of compression from Tertiary to recent time in the study area, although there is an anticlockwise rotation of the compression through time (over  $\sim 56$  Ma). Fault slip date inversion also show an anticlockwise change of the compression from upper Cretaceous to Oligocene (Table 4). In upper Cretaceous the compressional direction is NE-SW, while in Oligocene it has rotated towards N. Although without the exact dating method,





the actual time of faulting cannot be well constrained. Inversion According to reconstructions of the long-term Afro-Arabian–Eurasian convergence paths (McQuarrie et al., 2003 [2]), the relative plate motion changed from N30°E (56–33 Ma) to N25°E (33–19 Ma), N09°E (19–10 Ma), and N05°E (last 10 Ma). We suggest that the variation in the compressional trend over time resulted from changes in the continental convergence path, but that it was also influenced by the local structural evolution, such as lateral propagation folds and the presence of several décollement horizons that allowed decoupling of deformation between the basement and sedimentary cover (Oveisi et al., 2007 [43]). Because the results that we have obtained from the inversion of the earthquake focal mechanism and the fault slip data are from the foreland gneissic basement and sedimentary cover, respectively, the relative consistency between the results suggests that the compression has little inhomogeneity in both the overburden and the basement. Consequently, there are few changes in the compressional trend between the upper crust and ductile Hormuz salt décollement horizon. A comparison between the GPS surface displacement (Vernant et al., 2004 [1]; Tavakoli et al., 2008 [44]) with the early Pliocene compression in the Fars area (~ 5 Ma) supports this suggestion.

## 6. Conclusion

- The compressional regimes obtained from the inversion of the fault-slip data and the earthquake focal mechanisms are mutually consistent with the convergence between the Afro-Arabian continent and Eurasian continent.

- In the study area within the Zagros Foreland Folded Belt (F-FOB), a comparison between the paleo-compression directions obtained from fault-slip data and recent compression directions obtained from earthquake focal mechanisms indicate that there was insignificant variation in the compression direction throughout time. However, an anticlockwise rotation in the direction of the principal compressional stress over time is compatible with the variation of Afro-Arabian and Eurasian continental collision path. However, the NW compression direction observed in the middle segment of the Kar-e-Bas fault is incompatible with an anticlockwise rotation.

- The compatibility of our results with those of Lacombe et al. (2006) and Navabpour et al. (2007) indicates that there is not a significant difference in the compression direction in the vicinity of the lateral fault zones compared to the other parts of the Zagros Orogenic Belt. Consequently, the lateral fault zones (Kar-e-Bas, Sabz-Pushan and Sarvestan fault zones) may have initiated as tear faults in the cover above the décollement horizon along the thrust (e.g., HZF and MFF), and in recent times, these fault zones act as strike-slip/dip-slip faults in both the basement and the sedimentary cover.

- The obliquity of the maximum principal stress into the fault trends reveal a typical stress partitioning of dip-slip and strike-slip motion in the Kazerun, Kar-e-Bas, Sabz-Pushan, and Sarvestan fault zones, that caused these fault zones behave as segmented strike-slip/dip-slip faults.

- The almost relative consistency in the compressional direction in both the sedimentary cover and the gneissic basement suggests there is no significant change in the crustal compressional trend between basement and cover.

- There are two sources of the fault activities either as pre-existing dip-seated reactivated faults or shallow seated faults of the decoupling or décollement of rheological weak evaporates in the study area.



## 6. References

- [1]-Vernant, Ph., Nilforoushan, F., Hatzfeld, D., Abbassi, M. R., Vigny, C., Masson, F., Nankali, H., Martinod, J., Ashtiani, A., Bayer, R., Tavakoli, F., and Chéry, J., 2004, **Present-day crustal deformation and plate kinematics in the Middle East constrained by GPS measurements in Iran and northern Oman**, *Geophysical Journal International*, 157, 381 – 398
- [2]-McQuarrie, N., Stock, J. M., Verdel, C., and Wernicke, B. P., 2003, **Cenozoic evolution of Neotethys and implications for the causes of plate motions**, *Geophysical Research Letters*, 30, 20: SDE 6.1-SDE 6.4
- [3]-Lacombe, O., 2012, **Do fault slip data inversions actually yield paleostresses that can be compared with contemporary stresses? A critical discussion**, *Comptes Rendus Geoscience*, 344, 159–173
- [4]-Navabpour, P., Angelier, J., and Barrier, E., 2007, **Cenozoic post-collisional brittle tectonic history and stress reorientation in the High Zagros Belt (Iran, Fars Province)**, *Tectonophysics* 432, 101–131
- [5]-Mukherjee, S., 2013, **Channel flow extrusion model to constrain dynamic viscosity and Prandtl number of the Higher Himalayan Shear Zone**, *International Journal of Earth Sciences* 102, 1811-1835
- [6]-Huber, H., 1977, **Geological map of Iran, 1:1,000,000 with explanatory note**, National Iranian Oil Company. Exploration and Production Affairs, Tehran
- [7]- Berberian, M., 1995, **Master blind thrust faults hidden under the Zagros folds: active basement tectonics and surface tectonics surface morphotectonics**, *Tectonophysics* 241:193–224
- [8]-Sepéhr, M., and Cosgrove, J. W., 2005, **Role of the Kazerun Fault Zone in the formation and deformation of the Zagros fold-thrust belt, Iran**, *Tectonics*, 24, doi: 10.1029/2004TC001725
- [9]-Sarkarinejad, K., and Ghanbarian, M. A., 2014, **The Zagros hinterland fold-and-thrust belt in-sequence thrusting, Iran**, *Journal of Asian Earth Sciences* 85, 66–79
- [10]-Sarkarinejad, K., and Zafarmand, B., 2017a, **Tectonic stress and kinematic analyses of the Ghir fault zone, Zagros, Iran**. *Persian Geosciences*, 26, 102, 185-196
- [11]-Sarkarinejad, K., and Zafarmand, B., 2017b, **Stress state and movement potential of the Kar-e-Bas fault zone, Fars, Iran**. *Journal of Geophysics and Engineering*, 14, 998-1009
- [12]-Falcon, N., 1974, **Zagros Mountains, Mesozoic-Cenozoic orogenic belts, in Mesozoic Cenozoic Orogenic Belts: Data for Orogenic Studies**, collated and edited by A. M. Spencer, Geological Society London, Special Publications 4, 199 – 211
- [13]-Berberian, M., and King, G. C. P., 1981, **Towards a paleogeography and tectonic evolution of Iran**, *Canadian Journal of Earth Sciences* 18, 210 – 265
- [14]-Alavi, M., 1994, **Tectonics of the Zagros orogenic belt of Iran: new data and interpretations**, *Tectonophysics*, 229, 211–238
- [15]-Molinaro, M., Leturmy, P., Guezou, J. C., Frizon de Lamotte, D., and Eshraghi, S. A., 2005, **The structure and kinematics of the southeastern Zagros foldthrust belt, Iran: From thin-skinned to thick-skinned tectonics**, *Tectonics*, 24, TC3007, doi:10.1029/ 2004TC001633



- [16]-Lacombe, O., Mouthereau, F., Kargar, S., and Meyer, B., 2006, **Late Cenozoic and modern stress fields in the western Fars (Iran): implications for the tectonic and kinematic evolution of central Zagros**, *Tectonics*, 25, TC1003
- [17]-Aubourg, C., Smith, B., Eshraghi, A., Lacombe, O., Authemayou, C., Amrouch, K., Bellier, O., and Mouthereau, F., 2010, **New magnetic fabric data and their comparison with stress/strain markers from the Western Fars arc (Zagros); tectonic implications. In "Tectonic and Stratigraphic evolution of Zagros and Makran during the Meso-Cenozoic**, Geology Society, London, Spec. Publ., 330, 97-120
- [18]-Bayer, R., Chery, J., Tatar, M., Vernant, P., Abbassi, M., Masson, F., Nilforoushan, F., Doerflinger, E., Regard, V., and Bellier, O., 2003, **Active deformation in Zagros- Makran transition zone inferred from GPS measurements**, Fourth International Conference of Earthquake Engineering and Seismology, Tehran, Iran
- [19]-DeMets, C., Gordon, R. G., Argus, D. F., and Stein, S., 1990, **Current plate motions**, *Geophysical Journal International*, 101, 425–478
- [20]-Tatar, M., Hatzfeld, D., Martinod, J., Walpersdorf, A., Ghafari-Ashtiany, M., and Chéry, J. , 2002, **The present-day deformation of the central Zagros from GPS measurements**, *Geophysical Research Letters*, 29, 331–334
- [21]-Yamini-Fard, F., Hatzfeld, D., Tatar, M., and Mokhtari, M., 2006, **Microseismicity at the intersection between the Kazerun fault and the Main Recent Fault (Zagros-Iran)**, *Geophysical Journal International*, 166, 186–196
- [22]-Sherkati, S., and Letouzey, J., 2004, **Variation of structural style and basin evolution in the central Zagros (Izeh zone and Dezful embayment): Iran**, *Marine and Petroleum Geology*, 21, 535– 554
- [23]-Oveisi, B., Lavé, J., Beek, P., Carcaillet, J., Benedetti, L., and Aubourg, C., 2009, **Thick- and thin-skinned deformation rates in the central Zagros simple folded zone (Iran) indicated by displacement of geomorphic surfaces**, *Geophysical Journal International*, 176, 627-654
- [24]-Hessami, K., Nilforoushan, F., and Talbot, C. J., 2006, **Active deformation within the Zagros Mountains deduced from GPS measurements**, *Journal of the Geological Society*, London, 163, 143–148
- [25]-Sarkarinejad, K, and Azizi, A., 2008, **Slip partitioning and inclined dextral transpression along the Zagros Thrust System**, *Iran. Journal of Structural Geology*, 30, 116–136
- [26]-McKenzie, D. P., 1969, **The relation between fault plane solutions for earthquakes and the directions of the principal stresses**, *Bulletin of the Seismological Society of America*, 59, 591–601
- [27]-Otsubo, M., Yamaji, A., and Kubo, A., 2008, **Determination of stresses from heterogeneous focal mechanism data: An adaptation of the multiple inverse method**, *Tectonophysics*, 457, 150–160
- [28]-Yamaji, A., Sato, K., and Otsubo, M., 2011, **Multiple Inverse Method Software Package**, User's guide, 1-37
- [29]-Angelier, J., 1990, **Inversion of field data in fault tectonics to obtain the regional stress: III-A new rapid direct inversion method by analytical means**, *Geophysical Journal International*, 103, 363 – 376



- [30]-Zalohar, J., and Vrabec, M., 2007, **Paleostress analysis of heterogeneous fault slip data: the Gauss method**, *Journal of Structural Geology*, 29, 11, 1798–1810
- [31]-Wallace, R. E., 1951, **Geometry of shearing stress and relation to faulting**, *The Journal of Geology* 59, 118–130
- [32]-Bott, M. H. P., 1959, **The mechanisms of oblique-slip faulting**, *Geological Magazine*, 96, 109–117
- [33]-Twiss, R. J., and Unruh, J. R., 1998, **Analysis of fault slip inversions: Do they constrain stress or strain rate?**, *Journal of Geophysical Research*, 103, 12205 – 12222.
- [34]-Fossen, H., 2016, **Structural Geology**, Cambridge University Press New York, 2nd edition 1-463
- [35]-Hatzfeld, D., 1999, **The present-day tectonics of the Aegean as deduced from seismicity**, Geological Society, London, Special Publications 156, 1, 415-426.
- [36]-Maggi, A., Priestley, K., and Jacson, J., 2002, **Focal depths of moderate and large size earthquakes in Iran**, *Journal of Seismology and Earthquake Engineering*, 4, 1-10
- [37]-Talebian, M., and Jackson, J. A., 2004, **A reappraisal of earthquake focal mechanisms and active shortening in the Zagros mountains of Iran**, *Geophysical Journal International*, 156, 506–526.
- [38]-Tatar, M., Hatzfeld, D., and Ghafari-Ashtiany, M., 2004, **Tectonics of the central Zagros (Iran) deduced from microearthquakes seismicity**, *Geophysical Journal International*, 156, 255–266.
- [39]-Hatzfeld, D., Authemayou, C., Van der Beek, P., Bellier, O., Lavé, J., Oveisi, B., Tatar, M., Tavakoli, F., Walpersdorf, A., and Yamini-Fard, F., 2010, **The kinematics of the Zagros Mountains (Iran), in Tectonic and Stratigraphic Evolution of Zagros and Makran during the Mesozoic-Cenozoic**, edited by P. Leturmy and C. Robin, Geological Society London Special Publications 330, 19–42
- [40]-Sarkarinejad, K., Zafarmand, B. and Oveisi, B., 2018, **Evolution of the stress fields in the Zagros Foreland Folded Belt using focal mechanisms and kinematic analyses: the case of the Fars salient, Iran**, *International Journal of Earth Science*, 107, 611–633.
- [41]-Anderson, E. M., 1951, **The Dynamic of Faulting**, Edinburgh. Oliver and Boyd, 2nd Edition, Edinburgh, 133147
- [42]-Walpersdorf, A., Hatzfeld, D., Nankali, H., Tavakoli, F., Nilforoushan, F., Tatar, M., Vernant, P., Chery, J., and Masson, F., 2006, **Difference in the GPS deformation pattern of north and central Zagros (Iran)**, *Geophysical Journal International*, 167, 1077–1088
- [43]-Oveisi, B., Lavé, J., and Beek, P., 2007, **Rates and processes of active folding evidenced by Pleistocene terraces at the Central Zagros Front (Iran)**, *Thrust Belts and Foreland Basins Frontiers in Earth Sciences*, Springer Berlin Heidelberg, part V, 267-287
- [44]- Tavakoli, F., Walpersdorf, A., Authemayou, C., Nankali, H. R., Hatzfeld, D., Tatar, M., Djamour, Y., Nilforoushan, F., and Cotte, N., 2008, **Distribution of the right-lateral strike-slip motion from the Main Recent Fault to the Kazerun Fault System (Zagros, Iran): Evidence from present-day GPS velocities**, *Earth and Planetary Science Letters*, 276, 342-347.